COMMUNICATION

Journal of Materials Chemistry
www.rsc.org/materials

Biosynthesis of zirconia nanoparticles using the fungus *Fusarium oxysporum*

Vipul Bansal, Debabrata Rautaray, Absar Ahmad and Murali Sastry*

Materials Chemistry and Biochemical Science Division, National Chemical Laboratory, Pune – 411 008, India. E-mail: sastry@ems.ncl.res.in

Received 25th May 2004, Accepted 16th September 2004
First published as an Advance Article on the web 5th October 2004

Zirconia nanoparticles may be produced by challenging the fungus *Fusarium oxysporum* with aqueous ZrF_6^{2-} anions; extra-cellular protein-mediated hydrolysis of the anionic complexes results in the facile room temperature synthesis of nanocrystalline zirconia. Extracellular hydrolysis of the metal anions by cationic proteins of molecular weight around 24 to 28 kDa, which are rather similar in nature to silicatein, is shown to be responsible for the synthesis of zirconia nanoparticles, opening up the exciting possibility of large-scale biological synthesis of technologically important oxide materials.

There are innumerable examples in biology of exquisite hierarchically assembled inorganic structures synthesized under mild pH, pressure and temperature conditions. Classical examples of such processes include magnetotactic bacteria (magnetite nanoparticles),[1,2] diatoms (siliceous materials)[3–5] and S-layer bacteria (gypsum and calcium carbonate layers).[6] Silica formation in diatoms/sponges proceeds by hydrolysis of silicic acid by proteins such as silicatein[3] and polycationic peptides termed silaffins,[4] while laboratory-based synthesis of important oxides involves chemical transformation of their precursors under extreme temperature and pH conditions. While purely biological[3,4] and bioinspired[1,7] methods for the synthesis of oxides provide environmentally benign and energy-conserving processes, they have not been extended to the formation of other oxides such as zirconia.

Zirconia is a technologically promising oxide of interest as a structural and functional material.[8] Because of its intrinsic physicochemical properties such as hardness, shock wear, strong acid and alkali resistance, low frictional resistance, and high melting temperature, zirconia can be used as an abrasive, as a hard, resistant coating for cutting tools, and in high temperature engine components.[9] For these reasons, it is often called ceramic steel.[10] Zirconia nanoparticles are of great interest due to their improved optical and electronic properties with application as a piezoelectric, electro-optic and dielectric material.[8] Zirconia is also emerging as an important class of catalyst.[11] The synthesis of zirconia has been realized by physico-chemical methods such as sol–gel synthesis,[12] aqueous precipitation,[13] thermal decomposition[14] and hydrothermal synthesis.[15] However, all these methods require extremes of temperature (in the case of thermal synthesis) and pressure (hydrothermal synthesis). Rapid solid-state metathesis reactions[16] have proven to be quite successful, but have limited application due to the high temperature of operation and high cost. Biological methods for material synthesis would help circumvent many of the above detrimental features by enabling synthesis at mild pH, pressure and temperature and at a substantially lower cost.[1,7]

We discuss here our finding that exposure of the fungus *Fusarium oxysporum* to an aqueous solution of K_2ZrF_6 results in the protein-mediated extracellular hydrolysis of the zirconium hexafluoride anions and the room temperature formation of crystalline zirconia nanoparticles. *Fusarium oxysporum* is a plant pathogen and during its life cycle is not exposed to such ions. That this fungus should secrete proteins capable of hydrolyzing ZrF_6^{2-} complexes is unexpected, but has significant potential for development. The use of non-mineral forming microorganisms in advanced materials synthesis opens up possibilities for the commercially viable biological synthesis of technologically important oxides and semiconductors.

The plant pathogenic fungus *Fusarium oxysporum* was cultured as described elsewhere.[17] After incubation, the fungal mycelia was harvested and washed thoroughly under sterile conditions. A 20 g wet weight of the fungal biomass was then resuspended in 100 ml of a 10^{-3} M aqueous solution of K_2ZrF_6 (pH 3.6) in a 500 ml Erlenmeyer flask and kept on a shaker (200 rpm) at 27 °C. The reaction between the fungal biomass and ZrF_6^{2-} ions was carried out for a period of 24 h and the bio-transformed product formed was collected by separating the fungal mycelia from the aqueous extract by filtration under sterile conditions.

Representative bright and dark field transmission electron microscopy (TEM)[18] images from the fungus–K_2ZrF_6 reaction medium after 24 h of reaction are shown in Figs. 1A and B

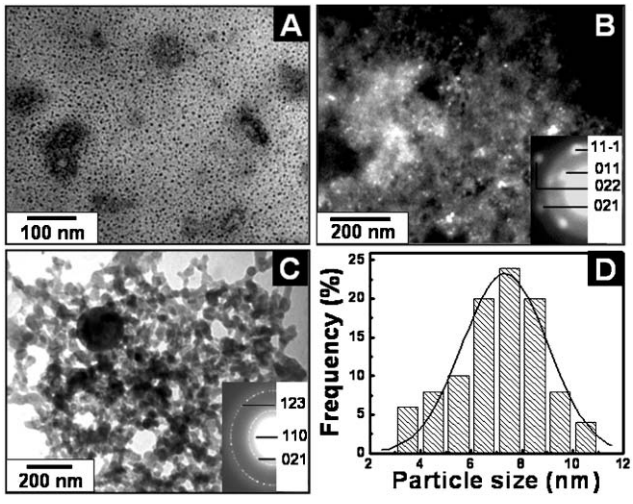

Fig. 1 A and B. Bright and dark field TEM micrographs recorded from zirconia nanoparticles synthesized using *Fusarium oxysporum* before calcination. C. Bright field TEM image recorded from the biogenic zirconia nanoparticles after calcination at 600 °C for 3 h. The insets in B and C correspond to the SAED patterns recorded from the representative zirconia nanoparticles shown in the main part of the figure [*d*-values : 3.69 Å (011); 3.63 Å (110); 3.16 Å ($11\bar{1}$); 2.61 Å (022); 2.32 Å (021); 1.34 Å (123)]. The TEM images were obtained on a JEOL 1200 EX instrument operated at an accelerating voltage of 120 kV. D shows a plot of the particle size distribution histogram of the zirconia nanoparticles synthesized by the fungus before calcination. The solid line is a Gaussian fit to the histogram.

DOI: 10.1039/b407904c

respectively. The particles are fairly regular in shape, presenting an overall quasi-spherical morphology (Fig. 1A). The particle size histogram shows that the particles range in size from 3 to 11 nm with an average size of 7.3 $\pm$ 2.0 nm (Fig. 1D). Selected area electron diffraction (SAED) analysis of the individual particles (inset, Fig. 1B) indicated that they were crystalline and revealed the monoclinic phase of ZrO_2. This is in agreement with X-ray diffraction (XRD)[18] analysis of films of the particles solution-cast from the fungus–K_2ZrF_6 reaction medium on glass substrates (Fig. 2A, curve 1), which show well-defined Bragg reflections characteristic of crystalline zirconia. Fourier transform infrared (FTIR)[18] analysis of particles from the fungus–ZrF_6^{2-} reaction medium taken in KBr pellets showed the presence of a prominent resonance at 613 cm^{-1} (Fig. 2B, curve 2). The strong 613 cm^{-1} band is attributed to excitation of the Zr–O–Zr stretching mode vibration,[19] which is absent in the spectrum of pure K_2ZrF_6 (Fig. 2B, curve 1). The presence of the absorption band at 819 cm^{-1} indicates the presence of the monoclinic Zr–O–Zr bending vibration.[19] Two absorption bands centered at 1655 and 1544 cm^{-1} (amide I and II bands respectively (Fig. 2C, curve 2) attest to the presence of proteins in the quasi-spherical particles, which are clearly missing in the K_2ZrF_6 sample (Fig. 2C, curve 1).

The TEM, FTIR, SAED and XRD analysis of the products of the reaction between K_2ZrF_6 with *Fusarium oxysporum* indicate the formation of crystalline ZrO_2 nanoparticles with a fairly large amount of proteins occluded into their structures. The biogenic ZrO_2 powder was then calcined in air at 300 °C for 3 h to remove the occluded proteins and promote crystallization of the oxides. The TEM images of the ZrO_2 particles show a dramatic change in the overall particle morphology after calcination (Fig. 1C). It is observed that the particles show greater contrast, indicating sintering and formation of denser zirconia particles (Fig. 1C). The discrete, individual particles observed in the as-prepared ZrO_2 particles (Figs. 1A and B) have given way to a more aggregated structure in which the individual particles can barely be discerned (Fig. 1C). SAED analysis of the zirconia particles after calcination (inset, Fig. 1C) shows sharp ring patterns that could be indexed based on the monoclinic structure of ZrO_2.[20] This is mirrored in the XRD pattern of the calcined zirconia sample that shows intense Bragg reflections (Fig. 2A, curve 2) characteristic of the monoclinic phase (peaks marked with 'M') with a small percentage of the tetragonal phase of zirconia (peaks marked with 'T'). It is clear from the XRD results that calcination improves the crystallinity of zirconia. FTIR analysis of the biogenic zirconia powder after calcination (curves 3 in Figs. 2B and C respectively) shows a sharpening of the Zr–O–Zr vibrational bands (at 613 cm^{-1} and 819 cm^{-1}) that is accompanied by the disappearance of the protein amide I and II bands from the particles (Fig. 2C, curve 3). Thus, the removal of the occluded proteins by calcination improves the crystallinity of the biogenic zirconia particles.

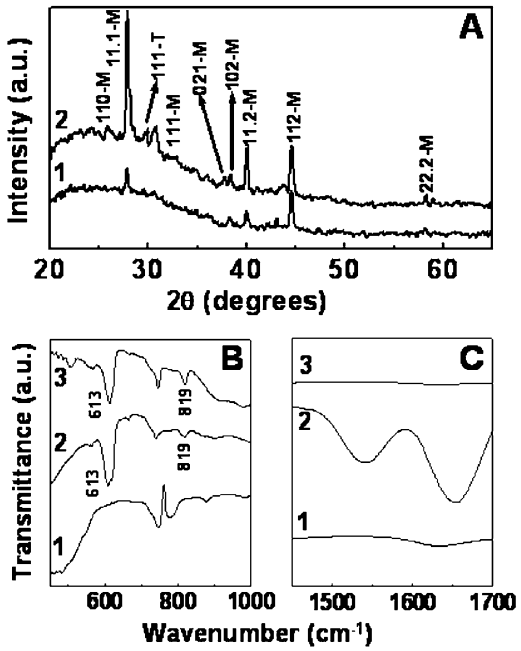

Fig. 2 A. XRD patterns recorded from zirconia nanoparticles synthesized by the reaction of aqueous K_2ZrF_6 with *Fusarium oxysporum*. Curves 1 and 2 correspond to the patterns recorded from the as-prepared and calcined zirconia samples respectively. The peaks marked with 'M' and 'T' correspond to the monoclinic and tetragonal phases of zirconia respectively. B. FTIR spectra recorded from powders of K_2ZrF_6 (curve 1); zirconia nanoparticles synthesized using *Fusarium oxysporum* before (curve 2) and after calcination at 600 °C for 3 h (curve 3). C. Expanded view of the FTIR spectra shown in B in the region of protein amide bands.

To identify the protein(s) secreted by the fungus *Fusarium oxysporum* that are responsible for hydrolysis of the aqueous anionic metal complexes, the extracellular proteins secreted by the fungus in the filtrate both in the absence and presence of ZrF_6^{2-} anions were concentrated by lyophilization and analyzed using 10% native and SDS-PAGE (sodium dodecyl sulfate polyacrylamide gel electrophoresis) carried out at pH 8.3. The differential expression profile of extracellular proteins secreted by *Fusarium oxysporum*, in the absence (Fig. 3A, lane 1) and presence of ZrF_6^{2-} ions (Fig. 3A, lane 2), when analyzed using native PAGE, clearly showed the induction of two extracellular proteins in the presence of ZrF_6^{2-} anions (bands highlighted by arrows in Fig. 3A). These two induced proteins were eluted from the gel and tested positive for hydrolysis of ZrF_6^{2-} ions to form nanozirconia. Similarly, a differential expression profile study of extracellular proteins secreted by *Fusarium oxysporum*, when carried out using SDS-PAGE (Fig. 3B) in the absence (Fig. 3B, lane 4) and presence of ZrF_6^{2-} ions (Fig. 3B, lane 5), along with standard protein molecular weight markers, showed the presence of at least two major bands centered around 24 and 28 kDa (bands highlighted by arrows in Fig. 3B). These protein bands, when eluted and checked on PAGE along with the proteins eluted from native PAGE, indicated that the corresponding two bands appear at the same level, thus suggesting that both

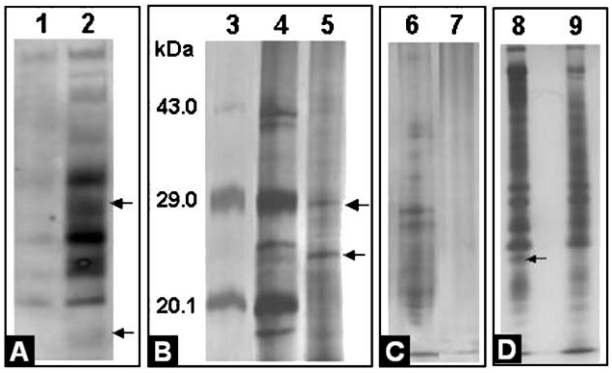

Fig. 3 A and B. The profile of extracellular proteins secreted by the *Fusarium oxysporum* biomass in the absence (lanes 1 and 4) and presence (lanes 2 and 5) of aqueous ZrF_6^{2-} ions, when run on a 10% native (panel A) and SDS-PAGE (panel B). Lane 3 shows the standard protein molecular weight markers with the corresponding molecular weights indicated. C. The profile of *Fusarium oxysporum* proteins bound to the zirconia nanoparticles run on SDS-PAGE after (lane 6) and before (lane 7) boiling in sodium dodecyl sulfate solution. D. The extracellular protein profile of *Trichothecium* sp. proteins obtained in the absence (lane 8) and presence (lane 9) of ZrF_6^{2-} ions, when run on 10% native PAGE. The arrows highlighting the bands in panels A and B indicate the proteins secreted by *Fusarium oxysporum* responsible for the hydrolysis of the ZrF_6^{2-} ions into zirconia nanoparticles, while the arrow in panel D indicates the protein whose expression is inhibited in *Trichothecium* sp. due to the presence of ZrF_6^{2-} ions.

proteins consist of monomeric units (data not shown for brevity). Further investigations are in progress to understand the individual role of the two proteins in zirconia formation, both in terms of the amino acid sequence of these proteins and the nature of their interaction with the zirconia particles.

The proteins bound to the surface of the biogenic zirconia nanoparticles were also analyzed in the following manner. The filtrate obtained after the reaction of ZrF_6^{-2} with the fungus *Fusarium oxysporum* was centrifuged at 15 000 rpm for 20 min and the precipitated zirconia nanoparticles were thoroughly washed with copious amounts of deionized water and analyzed on SDS-PAGE (Fig. 3C). To detach the surface-bound proteins from the nanoparticles, the ZrO_2 nanoparticles were boiled in 1% SDS solution for 5 min. Interestingly, when the SDS-treated (Fig. 3C, lane 6) and untreated nanoparticles (Fig. 3C, lane 7) were analyzed on 10% SDS-PAGE, the SDS-treated ZrO_2 nanoparticles showed a profile containing a large number of polypeptides (Fig. 3C, lane 6) while the profile of the untreated ZrO_2 nanoparticles did not show any proteins, apart from some smearing at the top of the gel (Fig. 3C, lane 7). The smearing might be due to the restricted entry of ZrO_2-bound proteins in the gel because of the large size of nanoparticles. This strongly suggests that the proteins bound to the ZrO_2 nanoparticles might be different from those that are responsible for the hydrolytic conversion of ZrF_6^{2-} ions to ZrO_2.

In order to determine the nature of the charge on the protein(s) responsible for hydrolysis of the zirconate anions, the filtrate obtained after reaction of the fungus *Fusarium oxysporum* with ZrF_6^{2-} anions was lyophilized, loaded on CM-Sephadex (a cation exchange matrix) and when the matrix-bound and unbound fractions were tested for activity, hydrolytic activity was observed only in the fraction that was bound to the matrix. This suggests that proteins responsible for hydrolytic activity are cationic in nature. Moreover, the cationic nature of these proteins was also confirmed using PAGE with reversed polarity of electrodes (data not shown for brevity).

The ZrF_6^{2-} anions are not toxic to the fungus *Fusarium oxysporum*, which can be extracted from the metal ion–fungus reaction medium and grown further in culture media. A number of other genera of fungi were tested for hydrolytic activity (*Trichothecium* sp., *Curvularia lunata, Colletotrichum gloeosporioides, Phomopsis* sp., *Aspergillus niger*), but did not yield positive results. The extracellular protein profile of *Trichothecium* sp. was studied in an attempt to increase our understanding behind the process. As in the case of *Fusarium oxysporum*, *Trichothecium* sp. was incubated both in the absence and presence of ZrF_6^{-2} ions and the respective filtrates were collected after 24 h of reaction. The filtrates obtained thereafter were concentrated by lyophilization and analyzed using 10% native PAGE. The differential expression profile of extracellular proteins secreted by *Trichothecium* sp., in the absence (Fig. 3D, lane 8) and presence of ZrF_6^{2-} ions (Fig. 3D, lane 9), when analyzed using native PAGE, did not show induction of additional extracellular proteins. Moreover, it showed the inhibition of an extracellular protein that expresses in *Trichothecium* sp. in the absence of ZrF_6^{2-} ions (band highlighted by arrow in Fig. 3D), which suggests that ZrF_6^{2-} ions might be inhibitory for the metabolism of *Trichothecium* sp. and some other similar fungi which do not show the hydrolytic activity for the conversion of metal oxide precursors to metal oxides.

In summary, we have shown here that the fungus *Fusarium oxysporum* secretes proteins capable of hydrolyzing aqueous ZrF_6^{2-} ions extracellularly to form zirconia at room temperature. Particularly gratifying is the fact that the fungus is capable of hydrolyzing tough metal halide precursors under acidic conditions. While the hydrolytic proteins secreted by *Fusarium oxysporum* are yet to be sequenced and studied for their role in the fungus metabolic pathways, our studies indicate that they are cationic proteins of molecular weight centered around 24 and 28 kDa and thus, similar to silicatein.[3] The regenerative capability of biological systems coupled with our finding that fungi such as *Fusarium oxysporum* are capable of hydrolyzing metal complexes that they never encounter during their growth cycle shows enormous promise for development, particularly in large-scale synthesis of metal oxides. The eco-friendly and energy-conserving nature of the fungus-based biological process for metal oxide synthesis in comparison with chemical processes such as the sol–gel method cannot be over-emphasized.

Acknowledgements

VB and DR thank the Council of Scientific and Industrial Research (CSIR) and Department of Science and Technology (DST), Government of India for research fellowships. The XRD and TEM facilities of the Centre for Materials Characterization, NCL, Pune are gratefully acknowledged.

Notes and references

1 R. Lovley, J. F. Stolz, G. L. Nord and E. J. F. Phillips, *Nature*, 1987, **330**, 252.
2 P. Philse and D. Maas, *Langmuir*, 2002, **18**, 9977.
3 K. Shimizu, J. Cha, G. D. Stucky and D. E. Morse, *Proc. Natl. Acad. Sci. U. S. A.*, 1998, **95**, 6234.
4 N. Kroger, R. Deutzmann, C. Bersdorf and M. Sumper, *Proc. Natl. Acad. Sci. U. S. A.*, 2000, **97**, 14133.
5 J. Milligan and F. M. M. Morel, *Science*, 2002, **297**, 1848.
6 U. B. Sleytr, P. Messner, D. Pum and M. Sara, *Angew. Chem., Int. Ed.*, 1999, **38**, 1034.
7 S. V. Patwardhan, N. Mukherjee, M. Steinitz-Kannan and S. J. Clarson, *Chem. Commun.*, 2003, 1122.
8 S. Somiya, N. Yamamoto and H. Yanagina, 'Science and Technology of Zirconia III', in *Advances in Ceramics*, American Ceramic Society, Westerville, OH, 1988, vols. 24A and 24B.
9 H. Heuer, *J. Am. Ceram. Soc.*, 1987, **70**, 689.
10 R. C. Garvey, R. H. Hannic and R. T. Pascoe, *Nature*, 1975, **258**, 703.
11 T. Yamaguchi, *Catal. Today*, 1994, **20**, 199.
12 H. Xu, D. Quin, Z. Yang and H. Li, *Mater. Chem. Phys.*, 2003, **80**, 524.
13 P. D. Southon, J. R. Baotlett, J. L. Woolfrey and B. Ben-Nissan, *Chem. Mater.*, 2002, **14**, 4313.
14 H. A. Raihani, B. Durand, F. Chassagneux, D. Kerridge and D. Inman, *J. Mater. Sci.*, 1994, **4**, 133.
15 H. Noh, D. Seo, H. Kim and J. Lee, *Mater. Lett.*, 2003, **57**, 2425.
16 E. G. Gillan and R. B. Kaner, *J. Mater. Chem.*, 2001, **11**, 1951.
17 P. Mukherjee, S. Senapati, D. Mandal, A. Ahmad, M. I. Khan, R. Kumar and M. Sastry, *ChemBioChem*, 2002, **3**, 461.
18 The samples for TEM were prepared by drop-coating on to a carbon-coated copper TEM grid. TEM and SAED patterns were obtained on a JEOL 1200 EX instrument operated at an accelerating voltage of 120 kV. FTIR spectroscopy of the purified and dried biogenic zirconia powder taken in KBr pellet was carried out on a Perkin-Elmer Spectrum One instrument at a resolution of 4 cm^{-1}. XRD measurements of drop-coated films of the biogenic zirconia on glass substrates before and after calcination were carried out on a Phillips PW 1830 instrument operated at a voltage of 40 kV and a current of 30 mA with Cu Kα radiation.
19 E. F. Lopez, V. S. Escribano, M. Panniza, M. M. Carnasciali and G. Busca, *J. Mater. Chem.*, 2001, **11**, 1891.
20 The XRD patterns were indexed with reference to the crystal structures from the ASTM charts: zirconia [ASTM chart card no. 2-0464 (monoclinic) and 2-0733 (tetragonal)].